ELSEVIER

Journal of Organometallic Chemistry 526 (1996) 175–183

Journal of Organometallic Chemistry

Substrate activation by the Wilkinson analogous complex ClRh(P ~ O)(P^O) containing η^2 P^O-chelated and η^1 P-bonded (methoxyethyl)dicyclohexylphosphine as a hemilabile ligand [1]

Ekkehard Lindner *, Berthold Keppeler, Hermann A. Mayer, Karlheinz Gierling, Riad Fawzi, Manfred Steimann

Institut für Anorganische Chemie der Universität Tübingen, Auf der Morgenstelle 18, D-72076 Tübingen, Germany

Received 23 May 1996

Abstract

In the presence of a variety of small molecules the pseudo 14-electron rhodium complex ClRh(P ~ O)(P^O) (1, P^O = $\eta^2(O,P)$-chelated $Cy_2PCH_2CH_2OCH_3$ ligand; P ~ O = $\eta^1(P)$-coordinated) is shown to undergo a facile cleavage of its intramolecular ether moiety. The reaction of 1 with ethene, diphenylacetylene and carbon disulfide results in the irreversible coordination of the corresponding molecule to the metal yielding the complexes $ClRh(C_2H_4)(P \sim O)_2$ (2), ClRh(PhC≡CPh)(P ~ O)$_2$ (3), $ClRhCS_2(P \sim O)_2$ (4), and ClRhCS(P ~ O)$_2$ (5). All compounds are obtained in excellent yields under very mild conditions. The structures of 4 and 5 were determined by single-crystal X-ray diffraction. The oxidative addition of HCl to the starting material 1 leads to the monochelated octahedrally coordinated complex $Cl_2Rh(H)(P \sim O)(P^O)$ (6). Complex 6 exhibits fluxional behavior on the ^{31}P NMR time scale. Line-shape analysis of variable temperature $^{31}P\{^1H\}$ NMR spectra of 6 affords the Eyring parameters $\Delta H^{\ddagger} = 42.3\,kJ\,mol^{-1}$ and $\Delta S^{\ddagger} = -63.7\,J\,mol^{-1}\,K^{-1}$, indicating an intramolecular exchange mechanism. The Rh–H bond in 6 is able to insert ethene to give the ethylrhodium(III) complex $Cl_2RhC_2H_5(P \sim O)_2$ (7). Subsequently, there follows a fast σ/π rearrangement to the complex $Cl_2Rh(\eta^2\text{-}C_2H_4)(H)(P \sim O)_2$ (8) which undergoes a slow π/σ transformation to the monochelated product $Cl_2Rh(C_2H_5)(P \sim O)(P^O)$ (9).

Keywords: Fluxionality; Oxidative addition; Phosphine; Rhodium; X-ray diffraction

1. Introduction

The interest in coordinatively unsaturated transition metal complexes stems from the fact that they represent highly reactive intermediates in catalytically operating processes and that they are able to coordinate and to activate a substrate molecule [1]. The introduction of bifunctional ether–phosphines (O,P) instead of 'classical' tertiary phosphines has significantly affected the isolation, and thus the examination, of coordinatively unsaturated species [2]. These ligands are provided with oxygen atoms incorporated in open-chain or cyclic ether moieties which form a weak metal–oxygen contact while the phosphorus atom is strongly coordinated to the central atom. From these 'hemilabile' ligands, it has been reported [2] that the ether oxygen donor may be regarded as an intramolecular solvent molecule stabilizing the vacant coordination site, hence making these complexes much more stable than simple solvent adducts. A range of (ether–phosphine)ruthenium and -palladium complexes exhibit fluxional behavior at rates slow enough to be studied by ^{31}P NMR spectroscopy [3,4]. Valuable thermodynamic data on the relative stability of metal–oxygen bonds could be obtained in this way. Recently, we reported on the dynamic behavior and the reactivity of the starting monochelated compound ClRh(P ~ O)(P^O) (1) toward H_2, O_2, and CH_3I [5]. It should be mentioned that the *iso*-propyl derivative of this complex was first published by Werner et al. [6]. In this paper our investigations are focused on the coordination and activation of small molecules with the *Wilkinson* analogous complex ClRh(P ~ O)(P^O) (1) (O,P = (2-methoxyethyl)dicyclohexylphosphine). Owing to the weak Rh–O interaction we are able to present

[1] Dedicated to Professor Cornelius Kreiter on the occasion of his 60th birthday.

* Corresponding author.

PII S0022-328X(96)06551-5

a reactive precursor having a vacant coordination site at the rhodium center. A facile Rh–O cleavage takes place if **1** is reacted with ethene, diphenylacetylene, and carbon disulfide. An oxidative addition of the substrate without cleavage of the Rh–O contact takes place if **1** is allowed to react with hydrogen chloride. All reactions proceed under very mild conditions with high selectivities of the desired products.

2. Results and discussion

2.1. Reaction of ClRh(P~O)(P^O) (1) with ethene, diphenylacetylene, and carbon disulfide

Recently we reported on the excellent catalytic activity of complex **1** in the hydrogenation of 1-hexene to *n*-hexane [5]. Consequently, we investigated the reactivity of **1** toward ethene as a model for the coordination of the olefin in a catalytic cycle. Treatment of **1** with C_2H_4 in dichloromethane at 273 K leads to an instant cleavage of the Rh–O contact resulting in the quantitative formation of the corresponding η^2-ethene complex **2** (Scheme 1). The η^2-coordination mode of the alkene to the rhodium center was proved by spectroscopic means. Its $^{31}P\{^1H\}$ NMR spectrum displays a doublet (Table 1), consistent with two equivalent trans phosphorus nuclei. This is confirmed by the appearance of virtual couplings for the PCH_2– and PCH–carbon atoms in the $^{13}C\{^1H\}$ NMR spectrum of **2** [7]. In addition, the $^{13}C\{^1H\}$ NMR spectrum of **2** shows a doublet at 38.5 ppm ($^1J(RhC) = 15.7$ Hz) being attributed to the carbon atoms of the ethene ligand. Compared with the similar complex $Rh(P(p\text{-tolyl})_3)_2(C_2H_4)Cl$ this signal is shifted 6 ppm to higher field, indicating the high electron density in **2** [8]. Accordingly, the analysis of the A_4 part of an A_4M_2X-type ^1H NMR spectrum for the ethene protons at 2.6 ppm affords the coupling constants $^2J(RhH) = 1.8$ Hz and $^3J(PH) = 4.0$ Hz. These values are well comparable with other η^2-ethene rhodium(I) complexes [6]. In contrast to the corresponding η^2-ethene rhodium(I) complex $Rh(PPh_3)_2(C_2H_4)Cl$, **2** does not eliminate ethene, neither in the solid state nor in solution [9].

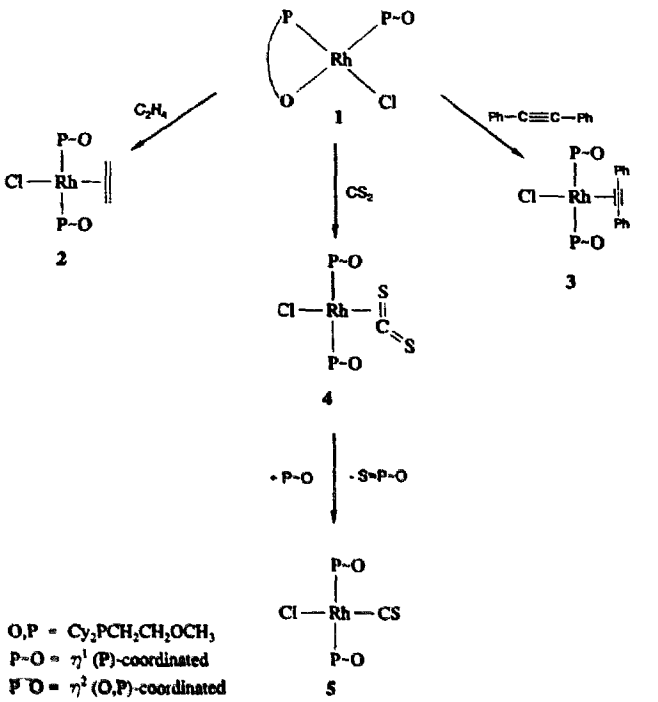

Scheme 1.

The interaction of **1** with stoichiometric amounts of diphenylacetylene in dichloromethane at 273 K afforded the η^2-diphenylacetylene complex **3** (Scheme 1), which is air-stable and readily soluble in polar organic solvents. Its $^{31}P\{^1H\}$ NMR spectrum shows a doublet for the two equivalent phosphorus atoms, indicating a square-planar geometry with trans-positioned phosphine ligands. The absorption of medium intensity at 1858 cm^{-1} in the IR spectrum of **3** is assigned to the C≡C stretching frequency. Compared with noncoordinated diphenylacetylene this band is shifted approximately 370 cm^{-1} toward lower energy. This points to a metallacyclopropene analogous coordination mode in **3** [6,10].

Table 1
$^{31}P\{^1H\}$ NMR and selected $^{13}C\{^1H\}$ NMR (chemical shifts δ ppm, coupling constants J Hz) and IR data (cm^{-1})

Complex	^{31}P NMR [a]			^{13}C NMR [b]		IR [c]
	δ	$^1J(RhP)$	$^2J(PP)$	CH_2O	OCH_3	$\nu_{as}(C_2O)$
2	18.6 (d)	121.3		69.8	58.4	1103 (m)
3	16.7 (d)	108.8		69.0	58.4	1104 (m)
4	28.2 (d)	132.3		70.3	58.5	1110 (m)
5	16.3 (d)	115.8		67.1	58.5	1106 (m)
6	59.4 (dd) [d]	126.9	24.2	71.2 [d]	61.5 [d]	1075 (m)
	53.3 (dd) [d]	146.3	24.2	68.0 [d]	58.5 [d]	1106 (m)
7	11.1 (d)	104.3		68.8	58.5	1106 (m)
8	31.2 (d)	97.2		70.4	59.7	1107 (m)
9	46.9 (dd)	131.2	19.5	69.2	59.2	1075 (m)
	38.4 (dd)	109.8	19.5	67.4	57.2	1105 (m)

[a] 101.25 MHz, C_6D_6, 295 K. [b] 62.90 MHz, C_6D_6, 295 K. [c] KBr. [d] CD_2Cl_2, 243 K.

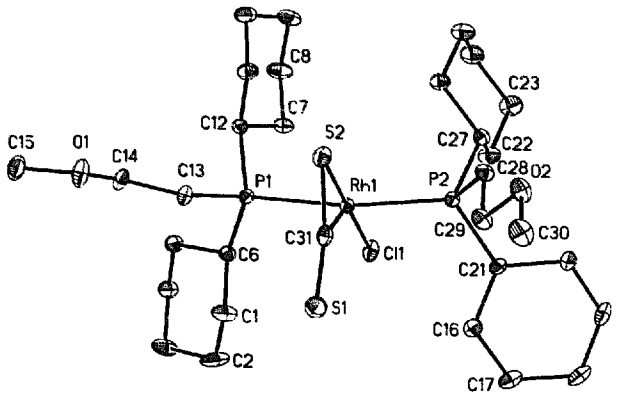

Fig. 1. ORTEP plot of the rhodium complex 4.

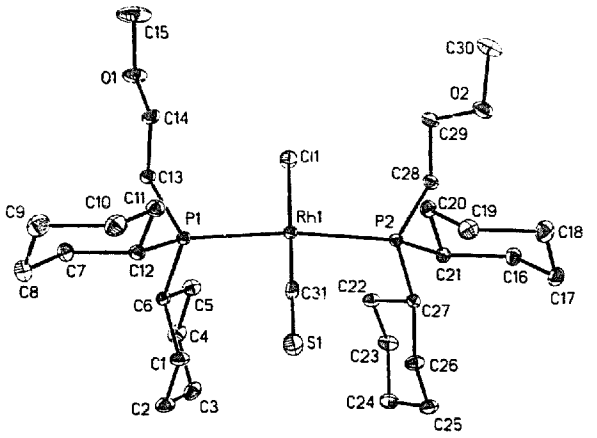

Fig. 2. ORTEP plot of the rhodium complex 5.

If the starting compound **1** is reacted with an excess of carbon disulfide in dichloromethane at 233 K the solution becomes dark brown and the yellow $\eta^2(C,S)$-carbon disulfide complex **4** is generated (Scheme 1). The $^{31}P\{^1H\}$ NMR spectrum of this CS_2 adduct displays a doublet (Table 1) which reveals two equivalent phosphorus atoms in trans position. In the $^{13}C\{^1H\}$ NMR spectrum the ^{13}C signal of the CS_2 group appears at 235.2 ppm as a low intensity doublet of triplets with the coupling constants $^1J(RhC) = 23.1$ Hz and $^2J(PC) = 4.2$ Hz respectively. Three IR absorptions at 1236, 1177, and 606 cm^{-1} are observed for the coordinated carbon disulfide. The position of these bands is well comparable with that of the similar complex $Rh(PCy_3)_2CS_2Cl$ [11].

An ORTEP plot of the molecular structure of **4** is shown in Fig. 1. A listing of selected bond distances and angles is given in Table 2. As expected from the chemical–physical characterization of the complex, the metal is five-coordinated by the two phosphorus functions of the phosphines, one chlorine atom, and by a CS_2 molecule through a C=S linkage.

The environment of the planar Rh–CS_2 fragment resembles that found in other metal complexes, containing a terminally η^2-bonded CS_2 group [12]. In particular the C–S(1) and C–S(2) bond lengths are somewhat longer than in carbon disulfide (1.554 Å, average) [13].

Table 2
Selected interatomic distances (Å) and angles (deg) for **4**

Bond lengths			
Rh(1)–P(1)	2.3752(11)	Rh(1)–C(31)	1.957(4)
Rh(1)–P(2)	2.3534(11)	S(2)–C(31)	1.675(4)
Rh(1)–S(2)	2.3662(11)	S(1)–C(31)	1.596(4)
Rh(1)–Cl(1)	2.3311(11)		
Bond angles			
P(1)–Rh(1)–P(2)	168.27(4)	C(31)–Rh(1)–Cl(1)	133.96(13)
Cl(1)–Rh(1)–P(1)	89.63(4)	C(31)–Rh(1)–S(2)	44.35(13)
Cl(1)–Rh(1)–P(2)	86.91(4)	P(1)–Rh(1)–S(2)	91.91(4)
C(31)–Rh(1)–P(1)	95.09(12)	S(1)–C(31)–S(2)	147.0(3)
C(31)–Rh(1)–P(2)	95.37(12)	S(2)–C(31)–Rh(1)	30.9(2)

The lengthening of both the C–S(1) and C–S(2) distances with respect to this molecule suggests that the $\eta^2(C,S)$-coordination of CS_2 reduces the bond order of both C–S bonds. This may result either from a charge transfer from the ligand to the metal or from an electron transfer from the metal to antibonding orbitals of the ligand. It is noteworthy that the S–C–S angle and the averaged value of the C–S bond lengths are very similar to the values found for carbon disulfide in the $^3A_2$ excited state (135° and 1.64 Å) [13].

The reaction of the η^2-CS_2 rhodium complex **4** with an excess of the O,P ligand $Cy_2PCH_2CH_2OCH_3$ in methanol at 273 K affords the thiocarbonyl rhodium complex **5** (Scheme 1). The $^{31}P\{^1H\}$ NMR spectrum of **5** consists of an A_2 part of an A_2X pattern which reveals two equivalent phosphorus atoms in trans position (Table 1). Accordingly, the analysis of the A part of an AMX_2-type $^{13}C\{^1H\}$ NMR spectrum of the highly shielded thiocarbonyl carbon atom at 274.3 ppm leads to the coupling constants $^2J(PC) = 14.4$ Hz and $^1J(RhC) = 69.2$ Hz. In the thiocarbonyl region the IR spectrum exhibits one strong band at 1285 cm^{-1}, which is shifted only 15 cm^{-1} toward lower energy compared with the related complex $Rh(PPh_3)_2(CS)Cl$ [14].

An ORTEP plot of the molecular structure of **5** is shown in Fig. 2. A listing of selected bond distances and angles is given in Table 3. As shown in Fig. 2, the rhodium atom has the expected square-planar coordina-

Table 3
Selected interatomic distances (Å) and angles (deg) for **5**

Bond lengths			
Rh(1)–P(1)	2.3455(10)	Rh(1)–C(31)	1.773(4)
Rh(1)–P(2)	2.3527(10)	S(1)–C(31)	1.561(4)
Rh(1)–Cl(1)	2.3764(10)		
Bond angles			
P(1)–Rh(1)–P(2)	170.51(3)	C(31)–Rh(1)–Cl(1)	178.04(13)
Cl(1)–Rh(1)–P(1)	89.94(4)	C(31)–Rh(1)–P(1)	90.20(12)
Cl(1)–Rh(1)–P(2)	90.67(3)	S(1)–C(31)–Rh(1)	179.2(3)

tion. The thiocarbonyl ligand is nearly linear. Compared with the uncoordinated CS_2 molecule, the carbon–sulfur distance appears to be slightly longer. According to the better π-acceptor and σ-donor properties of the CS ligand, the Rh–C distance is smaller than in the corresponding carbonyl rhodium(I) complex [15].

2.2. Reaction of ClRh(P ~ O)(P^O) (1) with HCl

Upon treatment of an orange solution of **1** with hydrogen chloride in diethyl ether at 273 K the octahedrally configured dichloro(hydrido)rhodium complex **6** can be isolated as a pale yellow compound (Scheme 2). The $^{31}P\{^1H\}$ NMR spectrum of **6** displays the AB part of an ABX pattern for the two different phosphine ligands at 243 K. Owing to its incorporation into a five-membered ring, the phosphorus atom of the chelated ligand resonates at lower field [16]. The $^2J(PP)$ coupling constant was found to be in the typical range for a cis arrangement of the two phosphorus nuclei. The hydride ligand shows the A part of an AMXY system in the ^1H NMR spectrum at −17.0 ppm ($^1J(RhH) = 19.7$ Hz, $^2J(PH) = 12.2$, 18.3 Hz).

Complex **6** shows a nonrigid behavior which was demonstrated by variable-temperature $^{31}P\{^1H\}$ NMR spectroscopy (Fig. 3). The observed dynamic phenomena are reversible. At low temperatures (below 253 K in toluene) the spectrum displays well-resolved doublets of doublets. As the temperature is raised, the two phosphorus doublet–doublet resonances first become broad and then slowly coalesce; finally, at 309 K, the typical A part of an A_2X spin system is observed. This averaging of the magnetic environments on the ^{31}P NMR time scale at this temperature indicates a rapid mutual exchange of two ether moieties. Both simulated and experimental spectra are depicted in Fig. 3.

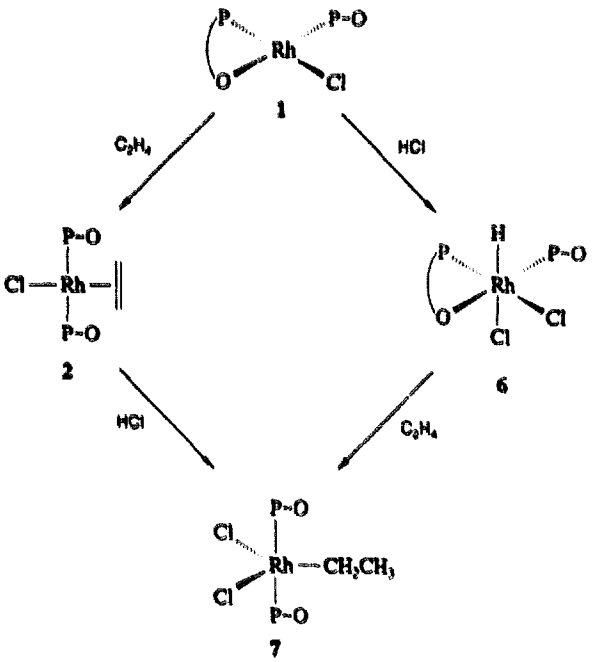

Scheme 2.

The analysis of the kinetic data with the Eyring equation affords the thermodynamic parameters $\Delta H^{\ddagger}$, $\Delta S^{\ddagger}$, $\Delta G_c^{\ddagger}$ and $\Delta G_{298}^{\ddagger}$ (see Table 4). $\Delta G^{\ddagger}$ is regarded as the difference between the ground and transition state. The negative value of $\Delta S^{\ddagger}$ is consistent with an ordered transition state which indicates an intramolecular exchange [17,18]. In view of the required rearrangement of the ligands, which causes a retardation of the process and a higher energy barrier for the exchange, it is not surprising that the rate constants for the exchange process are lower compared with those of the starting complex **1** ($k_{292} = 680\,s^{-1}$) [5]. The value for $\Delta G_{298}^{\ddagger}$ is well comparable with that found for the nonrigid behavior of a monochelated trichlororhodium(III) species $[RhCl_3\{Ph_2PCH_2C(O)Ph\}\{Ph_2PCH_2C(O)Ph\}]$ with β-ketophosphines as hemilabile ligands [19].

2.3. Insertion of ethene into the Rh–H bond of $Cl_2RhH(P \sim O)(\widehat{P\ O})$ (6)

When a solution of the monochelated rhodium complex **6** in dichloromethane is stirred at room temperature under 1.5 bar ethylene pressure, the color of the solution turns from initial yellow to deep red within 2 h and the ethyl rhodium(III) complex **7** is generated (Scheme 2). The same complex is also accessible within a few seconds and in higher yields by treating the η^2-ethene rhodium(I) complex **2** with a hydrogen chloride saturated diethyl ether solution at 273 K (Scheme 2). According to the NMR spectra and to the literature [20], complex **7** is five-coordinated with trans equivalent phosphine ligands in axial positions. Thus a doublet in the $^{31}P\{^1H\}$ NMR spectrum and a single set for the ether oxygen adjacent carbon atoms in the $^{13}C\{^1H\}$ NMR spectrum are observed (Table 1).

Owing to the CH_3 group the ^1H NMR spectrum of **7** shows a triplet centered at 0.8 ppm with a $^3J(HH)$ coupling constant of 6.4 Hz and an unresolved multiplet for the CH_2 protons at 2.8 ppm. The $^{13}C\{^1H\}$ NMR spectrum displays the resonances for the ethyl group at 16.6 ppm (d, $^1J(RhC) = 45.3$ Hz, $RhCH_2CH_3$) and 13.9 ppm (s, $RhCH_2CH_3$) (the assignment of the ^{13}C NMR resonances was supported by ^{13}C DEPT NMR spectroscopy [21]). In solution, even at low temperatures, complex **7** is transformed with β-hydrogen elimination into the isomeric octahedral dichloro(η^2-ethene)hydridorhodium(III) complex **8** (Scheme 3). Compound **8** is characterized by the appearance of a new doublet in the $^{31}P\{^1H\}$ NMR spectrum due to the two equivalent phosphorus ligands and a doublet of triplets at −24.5 ppm ($^1J(RhH) = 19.3$ Hz, $^2J(PH) = 13.5$ Hz) in the ^1H NMR spectrum for the generated hydride atom. A new doublet occurs in the $^{13}C\{^1H\}$

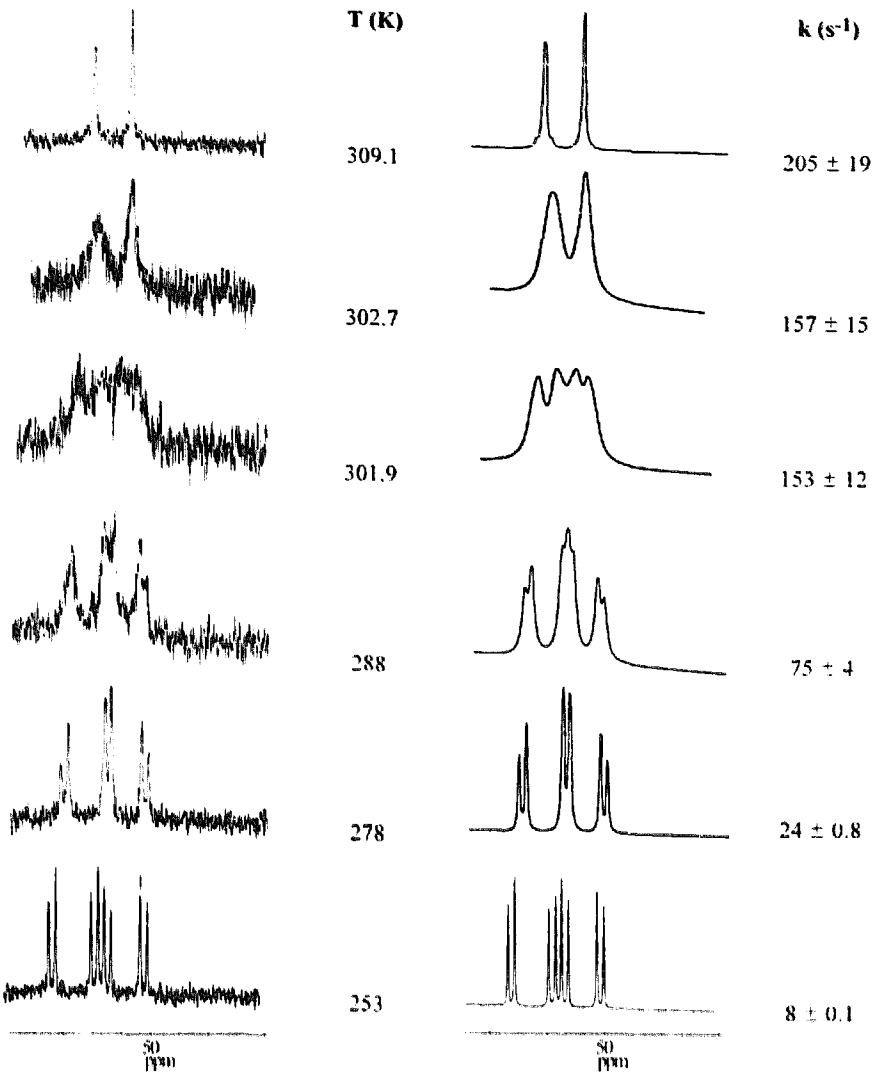

Fig. 3. Experimental (left) and simulated (right) variable-temperature $^{31}P\{^1H\}$ NMR spectra and rate constants k, for the mutual exchange of two different ether moieties of complex **6**.

NMR spectrum at 41.3 ppm ($^1J(RhC) = 28.1$ Hz) (the assignment of the ^{13}C NMR resonances was supported by ^{13}C DEPT NMR spectroscopy [21]) which is attributed to the coordinated ethene in **8**. This behavior in solution was not observed by Wilkinson and coworkers for the related PPh_3-substituted ethyl rhodium(III) complex, probably prevented by a reduced electron density in this rhodium complex [20]. After 12 h at room temperature a new set of signals is observed in the $^{31}P\{^1H\}$ NMR spectrum, which is assigned to the monochelated octahedral *cis*-ethyl rhodium(III) complex **9** (Scheme 3). This complex was characterized by its $^{31}P\{^1H\}$ and $^{13}C\{^1H\}$ NMR spectra (Table 1). The $^{13}C\{^1H\}$ NMR spectrum shows the signals for the ethyl carbon atoms at 16.6 ppm (d, $^1J(RhC) = 47.2$ Hz, $RhCH_2CH_3$) and 13.8 ppm (s, $RhCH_2CH_3$) (the assignment of the ^{13}C NMR resonances was supported by ^{13}C DEPT NMR spectroscopy [21]).

Table 4
Coalescence temperature and Eyring activation parameters for the fluxional process in **6**

Complex	T_c (K)	$\Delta H^{\ddagger a}$ (kJ mol^{-1})	$\Delta S^{\ddagger a}$ (J mol^{-1} K^{-1})	$\Delta G^{\ddagger b}$ (kJ mol^{-1})	$\Delta G^{\ddagger c}$ (kJ mol^{-1})
6	302	42.3 ± 2.3	−63.7 ± 8.1	61.5 ± 3.4	61.3 ± 2.4

[a] Calculated at coalescence temperature T_c using a modified version of DNMR5 and ACTPAR. [b] Calculated at T_c using the required law of propagation of errors. [c] Calculated at 298 K using the required law of propagation of errors.

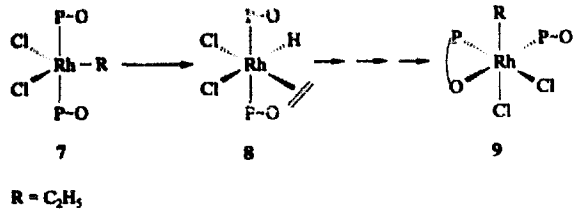

Scheme 3.

Compound **9** seems to be the thermodynamic product of the reactions between **6** and ethene, and **2** and hydrogen chloride. The direct transformation of **7** into **9** was not observed. In most cases no chelation of trans positioned ether–phosphines was observed. Obviously the β-hydrogen elimination in **7** is preferred. The generation of monochelated **9** by a π/σ transformation in **8** followed by a cis-orientation of the phosphines seems to be favored by the formation of a stable rhodium(III)–oxygen bond.

3. Conclusion

The starting compound **1**, which is closely related to the well-known Wilkinson catalyst represents a complex being stabilized by an intramolecular solvent. In view of the very weak Rh–O bond, **1** is regarded as a highly coordinatively unsaturated pseudo 14-electron complex. Hence, it can be anticipated to be a reactive precursor for the coordination of small molecules, which is an important step for the activation of such substrates in a rhodium-catalyzed reaction. This is nicely reflected by the reactions of **1** with hydrogen chloride and with ethene. The complexes **6**, **7**, **8**, and **9**, resulting from the consecutive sequence of oxidative addition of hydrogen chloride to **1**, and insertion of ethene into the Rh–H bond of **6** followed by an isomerization of **7** via **8** to **9**, represent a more stable system compared with the similar complexes generated by the reaction of **1** with dihydrogen and ethene. In this way the investigation of the catalytically important, and otherwise not detectable or even isolable, intermediates **6**, **7**, **8**, and **9** is enabled. These complexes can be regarded as models for a catalytic cycle. An insight into the metal–oxygen bond strength in complex **6** has been gained by detailed $^{31}P\{^1H\}$ DNMR spectroscopic experiments.

4. Experimental section

4.1. General procedures

All manipulations were carried out under an atmosphere of argon by use of standard Schlenk techniques. Solvents were dried over appropriate reagents and stored under argon. IR spectra were recorded on a Bruker IFS 48 FT-IR spectrometer. FD mass spectra were recorded on a Finnigan MAT 711 A instrument (8 kV, 333 K), modified by AMD; FAB mass spectra were obtained on a Finnigan MAT TSQ 70 (10 kV, 323 K). Elemental analyses were performed with a Carlo Erba 1106 analyzer and Perkin–Elmer Model 4000 atomic absorption spectrometer. Cl and S analyses were carried out according to Schöniger [22] and analyzed as described by Dirschel and Erne [23] and Wagner [24]. Rh was determined on a Perkin–Elmer Model 4000 atomic absorption spectrometer. ^1H, $^{31}P\{^1H\}$, $^{13}C\{^1H\}$ and ^{103}Rh NMR spectra were measured with a Bruker DRX 250 spectrometer at 250.13, 101.25, 62.90, and 7.90 MHz respectively. ^1H and ^{13}C chemical shifts were measured relative to partially deuterated solvent peaks and to deuterated solvent peaks respectively, which are reported relative to TMS. ^{31}P chemical shifts were measured relative to 85% H_3PO_4 ($\delta = 0$). The ^{103}Rh NMR resonances were measured using 2D (^{31}P, $^{103}Rh\{^1H\}$ and 2D (^1H, $^{103}Rh\{^{31}P\}$ experiments [25]. Chemical shift values are referred to $\Xi(Rh) = 3.16$ MHz [26]. $(C_6H_{11})_2PCH_2CH_2OCH_3$ [27] and the complex **1** were prepared as previously described [5].

4.2. ^{31}P DNMR

^{31}P DNMR investigations were performed on a Bruker AC 80 using a 10 mm o.d. NMR sample tube. The temperature was determined with a temperature control unit (Bruker VT 100 instrument) and an external thermocouple (PT 100). The NMR probe temperature was calibrated by the method of van Geet [28] and is considered accurate within ± 1 K (about 20 min was required for the temperature equilibration of the NMR sample). All exchange-broadened NMR spectra were simulated by applying a modified version of DNMR5 [29] available from Quantum Chemistry Program Exchange (QCMP No. 365). From the resulting rate constants the pertinent thermodynamic parameters were calculated with the nonlinear least squares program ACTPAR [30]. Reported values are given with the standard deviations.

4.3. Chlorobis[dicyclohexyl(methoxyethyl)phosphine-P](η²-ethene)rhodium(I) (2)

A solution of **1** (65 mg, 0.1 mmol) in 2 ml of dichloromethane was stirred at 273 K under an atmosphere of ethene (1 bar). The orange color of the solution turned immediately to bright yellow. The pale yellow solid was precipitated with 10 ml of *n*-hexane by cooling the solution to 203 K. The precipitate was collected, washed with *n*-hexane and dried in vacuo to yield 64 mg (95%) of **2**; m.p. 384 K (dec); MS (FD, 308 K) *m/e* 650 $[M^+ - C_2H_4]$. Anal. Found: C, 56.44; H, 9.42; Cl, 5.67; Rh, 15.43. $C_{32}H_{62}ClO_2P_2Rh$. Calc.:

C, 56.59; H, 9.20; Cl, 5.22; Rh, 15.15%. $^{13}C\{^1H\}$ NMR (62.90 MHz, C_6D_6, 295 K): δ 33.2 (vt, $N = 21$ Hz, [2] PCH), 30.6–25.0 (m, C_6H_{11}), 16.6 (vt, $N = 19$ Hz, [2] PCH_2). ^{103}Rh NMR (7.90 MHz, C_6D_6, 295 K): δ 271.

4.4. Chlorobis[dicyclohexyl(methoxyethyl)phosphine-P](η²-diphenylacetylene)rhodium(I) (3)

Addition of diphenylacetylene (18 mg, 0.1 mmol) to a solution of **1** (65 mg, 0.1 mmol) in 5 ml of dichloromethane at 273 K gave a bright yellow solution. An intensive yellow solid was precipitated with 10 ml of *n*-hexane by cooling the solution to 203 K. The solid was dried in vacuo to yield 77 mg (93%) of **3**; m.p. 399 K (dec.); MS (FD, 308 K) *m/e* 828 [M^+], Anal. Found: C, 63.90; H, 8.43; Cl, 4.37; Rh, 12.87. $C_{44}H_{68}ClO_2P_2Rh$. Calc.: C, 63.72; H, 8.26; Cl, 4.27; Rh, 12.41%. $^{13}C\{^1H\}$ NMR (62.90 MHz, C_6D_6, 295 K): δ 130.6–127.0 (m, C–Ph), 85.1 (d, $^1J(RhC) = 16.1$ Hz, C≡C) 34.4 (vt, $N = 22$ Hz, [2] PCH), 30.7–25.5 (m, C_6H_{11}), 21.1 (vt, $N = 20$ Hz, [2] PCH_2). ^{103}Rh NMR (7.90 MHz, C_6D_6, 295 K): δ 1120.

4.5. (Carbon disulfide-C,S)chlorobis[dicyclohexyl-(methoxyethyl)phosphine-P]rhodium(I) (4)

A solution of **1** (65 mg, 0.1 mmol) in 4 ml of dichloromethane was treated with carbon disulfide at 233 K. Instantaneously, the reaction mixture turned to dark brown. A yellow solid was precipitated at 203 K by treating the solution with 10 ml of *n*-hexane. The precipitate was washed with *n*-hexane and dried in vacuo to yield 68 mg (94%) of **4**; m.p. 357 K (dec.); MS (FD, 308 K) *m/e* 694 [$M^+ - S$]. Anal. Found: C, 51.20; H, 8.34; Cl, 5.10; Rh, 14.41; S, 8.87. $C_{31}H_{58}ClO_2P_2RhS_2$. Calc.: C, 51.20; H, 8.05; Cl, 4.88; Rh, 14.15; S, 8.82%. $^{13}C\{^1H\}$ NMR (62.90 MHz, C_6D_6, 295 K): δ 34.9 (vt, $N = 22$ Hz, [2] PCH), 29.8–26.9 (m, C_6H_{11}), 17.4 (vt, $N = 21$ Hz, [2] PCH_2). ^{103}Rh NMR (7.90 MHz, C_6D_6, 295 K): δ 2135.

4.6. Chlorobis[dicyclohexyl(methoxyethyl)phosphine-P](thiocarbonyl)rhodium(I) (5)

A solution of **4** (73 mg, 0.1 mmol) in 10 ml of methanol was reacted with 26 mg (0.1 mmol) of $(C_6H_{11})_2PCH_2CH_2OCH_3$ at 273 K. Almost immediately, the reaction mixture became dark green. After the solution was stirred for 2 h, the green color faded to orange-brown. A pale yellow solid was precipitated by cooling the solution to 203 K. The solid was washed with 5 ml of *n*-hexane and dried in vacuo to yield 52 mg (75%) of **5**; m.p. 399 K; MS (FD, 308 K) *m/e* 694 [M^+]. Anal. Found: C, 53.48; H, 8.44; Cl, 5.07; Rh, 14.48; S, 4.67. $C_{31}H_{58}ClO_2P_2RhS$. Calc.: C, 53.56; H, 8.41; Cl, 5.10; Rh, 14.83; S, 4.61%. $^{13}C\{^1H\}$ NMR (62.90 C_6D_6, 295 K): δ 34.4 (vt, $N = 25$ Hz, [2] PCH), 30.3–26.5 (m, C_6H_{11}), 21.0 (vt, $N = 25$ Hz, [2] PCH_2). ^{103}Rh NMR (7.90 MHz, C_6D_6, 295 K): δ 380.

4.7. Dichlorobis[dicyclohexyl(methoxyethyl)phosphine-P,O',P']hydridorhodium(III) (6)

A saturated solution of hydrogen chloride in diethyl ether (0.3 ml) was added to a solution of **1** (65 mg, 0.1 mmol) in 5 ml of diethyl ether at 273 K. The color of the solution immediately turned from orange to yellow. A pale yellow solid was precipitated by cooling the solution to 203 K and it was washed with 5 ml of diethyl ether. The solid was dried in vacuo to yield 64 mg (93%) of complex **7**; m.p. 369 K (dec.); MS (FD, 308 K) *m/e* 687 [M^+]. Anal. Found: C, 51.30; [3] H, 9.02; Cl, 10.23; Rh, 15.13. $C_{30}H_{59}Cl_2O_2P_2Rh$. Calc.: C, 52.41; H, 8.65; Cl, 10.31; Rh, 14.97%. $^{13}C\{^1H\}$ NMR (62.90 MHz, CD_2Cl_2, 233 K): δ 34.7 (m, PCH), 29.6–26.3 (m, C_6H_{11}), 25.5 (m, PCH_2). ^{103}Rh NMR (7.90 MHz, CD_2Cl_2, 295 K): δ 1287.

4.8. Dichlorobis[dicyclohexyl(methoxyethyl)phosphine-P](ethyl)rhodium(III) (7)

4.8.1. Method A

A saturated solution of hydrogen chloride in diethyl ether (0.3 ml) is added to a solution of **2** (68 mg, 0.1 mmol) in 5 ml of diethyl ether at 273 K. The color of the solution immediately turned from yellow to red. A pale yellow solid was precipitated by cooling the solution to 203 K, and it was washed three times with 5 ml of *n*-hexane. The precipitate was dried in vacuo to yield 45 mg (63%) of complex **7**; m.p. 376 K (dec.); MS (FD, 308 K) *m/e* 685 [$M^+ - C_2H_4$]. Anal. Found: C, 52.02; [4] H, 8.66; Cl, 10.06; Rh, 14.03. $C_{32}H_{63}Cl_2O_2P_2Rh$. Calc.: C, 53.71; H, 8.87; Cl, 9.91; Rh, 14.38%. $^{13}C\{^1H\}$ NMR (62.90 MHz, C_6D_6, 295 K): δ 33.6 (vt, $N = 20$ Hz, [2] PCH), 30.9–24.7 (m, C_6H_{11}), 21.0 (vt, $N = 20$ Hz, [2] PCH_2).

4.8.2. Method B

A solution of **6** (69 mg, 0.1 mmol) in 5 ml of dichloromethane was stirred at ambient temperature under a pressure of 1.5 bar ethene until a red solution was obtained. The reaction takes approximately 2 h. A pale

[2] $N = |^1J_{PC} + {}^3J_{PC}|$ [31].

[3] Although high temperatures and V_2O_5 (catalyst) were used for C, H analyses, the carbon values remained low. This is probably due to incomplete combustion, which may be caused by rhodium [32].

[4] See footnote 3.

yellow solid was precipitated by treating the solution with 10 ml of *n*-hexane at 203 K and it was washed three times with 5 ml of *n*-hexane. The precipitate was dried in vacuo to yield 42 mg (59%) of **7**. The compound was characterized by its $^{31}P\{^1H\}$ NMR spectrum (101.25 MHz, C_6D_6, 295 K): δ 11.1 (d, ^1J(RhP) 104.3 Hz).

4.9. Crystallographic analyses

Single crystals of **4** were grown from a *n*-hexane solution at 243 K. Single crystals of **5** were obtained in methanol at 243 K. Both crystals were mounted on a glass fiber and transferred to a P4 Siemens diffractometer. Rotation photographs were taken and a photo search was performed to find a suitable reduced cell (graphite-monochromated Mo Kα radiation). The lattice constants were determined with 25 precisely centered high-angle reflections and refined by least squares methods. The final cell parameters and specific data collection parameters for **4** and **5** are summarized in Table 5. The atomic coordinates and equivalent isotropic displacement parameters for **4** and **5** are given in Tables 6 and 7. Intensities were collected with the ω-scan technique with scan speed varying from 8 to 30° min^{-1} in ω. Scan ranges for **4** and **5** were 0.8° and 1° respectively. An empirical absorption correction was performed (ψ-scan maximal and minimal transmission 0.502 and 0.459 (**4**) and 0.718 and 0.527 (**5**)). All structures were solved by the Patterson method [33] and refined by least squares with anisotropic thermal parameters for all non-hydrogen atoms. Hydrogen atoms were included in calculated positions (riding model). Maximum and minimum peaks in the final difference synthesis were respectively 0.767 and −0.873 e Å^{-3} (**4**), and 1.135 and −0.533 e Å^{-3} (**5**). The asymmetric unit of **4** contains half a molecule of *n*-hexane and that of **5** one molecule of methanol. Further details of the crystal structure investigations are available on request from the Fachinformationszentrum Karlsruhe, Gesellschaft für wissenschaftlich-technische Information mbH, D-76344

Table 5
Crystal data and collection parameters for **4** and **5**

Compound	**4**·0.5*n*-hexane	**5**·methanol
Formula	$C_{34}H_{63}ClO_3P_2RhS_2$	$C_{32}H_{63}ClO_3P_2RhS$
FW	770.28	727.18
Crystal size (mm^3)	0.20×0.25×0.35	0.25×0.25×0.50
Crystal system	monoclinic	monoclinic
Space group	$C2/c$	$C2/c$
a (Å)	19.730(3)	23.840(3)
b (Å)	14.250(2)	14.306(2)
c (Å)	27.629(4)	21.903(4)
β (deg)	93.11(2)	102.41(1)
V (Å^3)	7757(2)	7296(2)
Z	8	8
Calc. density (g cm^{-3})	1.319	1.324
T (K)	173	173
F(000), e	3272	3088
μ(Mo Kα) (mm^{-1})	0.727	0.715
Scan range (2θ) (deg)	4–50	4–50
No. of unique reflections	13660	12834
Obs. data ($I \geq 2\sigma(I)$)	4517	4363
No. of parameters	380	352
Goodness of fit	1.330	1.410
$R1$ [a]	0.038	0.035
$wR2$ [b]	0.085	0.078

[a] $R1 = \Sigma||F_o| - |F_c||/\Sigma|F_o|$. [b] $wR2 = [\Sigma[w(F_o^2 - F_c^2)^2]/(\Sigma[w(F_o^2)^2])^{0.5}$.

Table 6
Atomic coordinates (×10^4) of **4** with equivalent isotropic displacement coefficients (Å^2 ×10^3) [a]

Atom	x	y	z	U_{eq}
Rh(1)	4249(1)	3647(1)	−1247(1)	23(1)
S(1)	2624(1)	3830(1)	−1489(1)	47(1)
S(2)	3919(1)	3542(1)	−2082(1)	35(1)
Cl(1)	4543(1)	3795(1)	−422(1)	39(1)
P(2)	4489(1)	5258(1)	−1313(1)	25(1)
P(1)	4252(1)	1988(1)	−1162(1)	24(1)
O(1)	3285(2)	33(2)	−2028(1)	58(1)
O(2)	3476(2)	6621(2)	−2431(1)	41(1)
C(1)	3310(3)	1831(4)	−464(2)	51(1)
C(2)	3135(4)	1592(4)	55(2)	71(2)
C(3)	3287(3)	586(4)	183(2)	59(2)
C(4)	4016(3)	334(4)	89(2)	44(1)
C(5)	4178(3)	549(3)	−433(2)	39(1)
C(6)	4045(2)	1580(3)	−552(2)	29(1)
C(7)	5638(2)	1958(4)	−912(2)	38(1)
C(8)	6356(3)	1626(4)	−1013(2)	52(1)
C(9)	6535(2)	1842(4)	−1527(2)	52(1)
C(10)	6017(3)	1418(4)	−1887(2)	48(1)
C(11)	5296(2)	1737(4)	−1796(2)	40(1)
C(12)	5108(2)	1538(3)	−1275(2)	29(1)
C(13)	3673(2)	1371(3)	−1595(2)	33(1)
C(14)	3706(2)	311(3)	−1634(2)	40(1)
C(15)	3187(3)	−943(4)	−2066(2)	62(2)
C(16)	3461(2)	5854(3)	−701(2)	38(1)
C(17)	3280(3)	6468(4)	−276(2)	46(1)
C(18)	3394(3)	7500(4)	−378(2)	53(1)
C(19)	4131(3)	7670(3)	−496(2)	51(1)
C(20)	4324(3)	7072(3)	−921(2)	41(1)
C(21)	4197(2)	6029(3)	−827(2)	30(1)
C(22)	5777(2)	5415(4)	−801(2)	45(1)
C(23)	6543(3)	5548(4)	−826(2)	55(1)
C(24)	6850(3)	4823(4)	−1143(2)	53(1)
C(25)	6500(3)	4819(5)	−1649(2)	53(1)
C(26)	5740(2)	4686(4)	−1631(2)	38(1)
C(27)	5420(2)	5426(3)	−1307(2)	32(1)
C(28)	4255(2)	5859(3)	−1889(1)	30(1)
C(29)	3510(2)	6052(3)	−2013(2)	36(1)
C(30)	2797(3)	6818(4)	−2585(2)	47(1)
C(31)	3389(2)	3698(3)	−1635(2)	31(1)
C(32)	777(5)	3553(7)	−1449(4)	113(3)
C(33)	552(6)	3619(15)	−1918(5)	308(17)
C(34)	143(4)	3495(9)	−2261(3)	137(5)

[a] Equivalent isotropic U defined as one-third of the trace of the orthogonalized U_{ij} tensor.

Table 7
Atomic Coordinates ($\times 10^4$) of **5** with equivalent isotropic displacement coefficients ($Å^2 \times 10^3$) [a]

atom	x	y	z	U_{eq}
Rh(1)	−4058(1)	2992(1)	4173(1)	21(1)
Cl(1)	−3342(1)	1811(1)	4293(1)	39(1)
P(1)	−4746(1)	1861(1)	4271(1)	22(1)
P(2)	−3351(1)	4161(1)	4253(1)	22(1)
S(1)	−5072(1)	4638(1)	3937(1)	48(1)
O(1)	−4180(3)	−517(3)	3599(3)	56(2)
O(2)	−2441(2)	4107(4)	3181(2)	46(1)
C(1)	−5129(3)	2751(4)	5247(3)	35(2)
C(2)	−5205(4)	2737(5)	5928(3)	42(2)
C(3)	−4661(4)	2547(4)	6378(3)	44(2)
C(4)	−4393(3)	1632(5)	6225(3)	41(2)
C(5)	−4298(3)	1623(5)	5551(3)	36(2)
C(6)	−4865(3)	1836(4)	5084(2)	25(1)
C(7)	−5893(3)	1226(5)	3824(3)	34(1)
C(8)	−6493(3)	1437(6)	3437(3)	43(2)
C(9)	−6476(3)	1625(6)	2756(3)	45(2)
C(10)	−6060(3)	2401(5)	2698(3)	41(2)
C(11)	−5455(3)	2193(5)	3087(3)	32(1)
C(12)	−5473(2)	2006(5)	3770(2)	25(1)
C(13)	−4555(3)	636(4)	4171(3)	31(1)
C(14)	−4457(3)	368(4)	3545(3)	36(2)
C(15)	−4090(7)	−847(7)	3013(5)	91(4)
C(16)	−3068(3)	5905(4)	3787(3)	30(1)
C(17)	−3285(3)	6775(4)	3398(3)	35(2)
C(18)	−3532(3)	6511(5)	2722(3)	40(2)
C(19)	−4011(3)	5784(5)	2678(3)	35(2)
C(20)	−3793(3)	4905(4)	3057(3)	28(1)
C(21)	−3552(3)	5182(4)	3741(3)	25(1)
C(22)	−3129(3)	3874(4)	5543(3)	29(1)
C(23)	−2938(3)	4264(5)	6206(3)	38(2)
C(24)	−3359(3)	4990(5)	6336(3)	36(2)
C(25)	−3438(3)	5774(5)	5845(3)	38(2)
C(26)	−3612(3)	5397(5)	5182(3)	34(1)
C(27)	−3185(3)	4664(4)	5044(3)	25(1)
C(28)	−2625(3)	3794(4)	4193(3)	29(1)
C(29)	−2545(3)	3370(5)	3584(3)	36(2)
C(30)	−2317(4)	3765(7)	2621(4)	54(2)
C(31)	−4595(3)	3868(4)	4050(3)	32(1)

[a] Equivalent isotropic U defined as one-third of the trace of the orthogonalized U_{ij} tensor.

Eggenstein-Leopoldshafen, on quoting the depository numbers CSD-405244 (**4**) and CSD-405245 (**5**), the names of the authors and the journal citation.

Acknowledgements

Support of this work by the Fonds der Chemischen Industrie, Frankfurt/Main, Germany, and by Degussa AG is gratefully acknowledged.

References

[1] E. Lindner, M. Haustein, K. Fawzi, M. Steimann and P. Wegner, *Organometallics, 13* (1994) 5021.
[2] A. Bader and E. Lindner, *Coord. Chem. Rev., 108* (1991) 27.
[3] E. Lindner, A. Möckel, H.A. Mayer, H. Kühbauch, R. Fawzi and M. Steimann, *Inorg. Chem., 32* (1993) 1266.
[4] E. Lindner, J. Dettinger, H.A. Mayer, R. Fawzi and M. Steimann, *Chem. Ber., 126* (1993) 1317.
[5] E. Lindner, Q. Wang, H.A. Mayer, H. Kühbauch and P. Wegner, *Organometallics, 12* (1993) 3291.
[6] H. Werner, A. Hampp, K. Peters, E.M. Peters, L. Walz and H.G. von Schnering, *Z. Naturforsch. Teil B, 45* (1990) 1548.
[7] G.T. Andrews, I.J. Colquhoun and W. McFarlane, *Polyhedron, 8* (1983) 783.
[8] C.A. Tolman, P.Z. Meakin, D.L. Lindner and J.P. Jesson, *J. Am. Chem. Soc., 96* (1974) 2762.
[9] J.A. Osborn, F.H. Jardine, J.F. Young and G. Wilkinson, *J. Chem. Soc. A,* (1966) 1711.
[10] H. Werner, J. Wolf, U. Schubert and K. Ackermann, *J. Organomet. Chem., 317* (1986) 327.
[11] H.L.M. Gaal and J.P.J. Verlaan, *J. Organomet. Chem., 133* (1977) 93.
[12] C. Bianchini, D. Masi, C. Mealli, A. Meli and M. Sabat, *Organometallics, 4* (1985) 1014.
[13] B. Kleman, *Can. J. Phys., 41* (1963) 2034.
[14] M.C. Baird, G. Hartwell and G. Wilkinson, *J. Chem. Soc. A,* (1967) 2037.
[15] B. Keppeler, *Ph.D. Thesis*, University of Tübingen, 1996.
[16] E. Lindner, R. Fawzi, K. Eichele, H.A. Mayer and W. Hiller, *Organometallics, 11* (1992) 1033.
[17] A. Stanger and K.P.C. Vollhard, *Organometallics, 11* (1992) 317.
[18] J.R. Koe, H. Tobita, T. Suzuki and H. Ogino, *Organometallics, 11* (1992) 150.
[19] P. Braunstein, Y. Chauvin, J. Nähring and J. Fischer, *J. Chem. Soc. Dalton Trans.,* (1995) 863.
[20] M.C. Baird, J.T. Mague, J.A. Osborn and G. Wilkinson, *J. Chem. Soc. A,* (1967) 1347.
[21] H. Günther (ed.), *NMR-Spektroskopie*, Thieme, Stuttgart, 1992.
[22] (a) W. Schöniger, *Microchim. Acta,* (1955) 123. (b) W. Schöniger, *Microchim. Acta,* (1956) 869.
[23] A. Dirschel and F. Erne, *Microchim. Acta,* (1961) 866.
[24] S. Wagner, *Microchim. Acta,* (1957) 19.
[25] R. Benn and Ch. Brevard, *J. Am. Chem. Soc., 108* (1986) 5622.
[26] B.E. Mann, in P.S. Pregosin (ed.), *Transition Metal Nuclear Magnetic Resonance*, Elsevier, Amsterdam, 1991.
[27] E. Lindner, S. Meyer, P. Wegner, B. Karle, A. Sickinger and B. Steger, *J. Organomet. Chem., 335* (1987) 59.
[28] (a) A.L. Van Geet, *Anal. Chem., 40* (1968) 2227. (b) A.L. Van Geet, *Anal. Chem., 42* (1970) 679.
[29] H. Kühbauch, University of Tübingen, 1992.
[30] G. Binsch and H. Kessler, *Angew. Chem. Int. Ed. Engl., 19 (1980) 411* and references cited therein.
[31] R.K. Harris, *Can. J. Chem., 42* (1964) 2275.
[32] T.E. Nappier, D.W. Meek, R.M. Kirchner and J.A. Ibers, *J. Am. Chem. Soc., 95* (1973) 4194.
[33] G.M. Sheldrick, SHELXTL *5.03 program*, University of Göttingen, 1995.